Selective mitochondrial superoxide generation *in vivo* is cardioprotective through hormesis

Salvatore Antonucci[1,*], John F. Mulvey[2,*], Nils Burger[3], Moises Di Sante[1], Andrew R. Hall[3], Elizabeth C. Hinchy[3], Stuart T. Caldwell[4], Anja V. Gruszczyk[3], Soni Deshwal[1], Richard C. Hartley[4], Nina Kaludercic[5], Michael P. Murphy[3], Fabio Di Lisa[1,5,+], Thomas Krieg[2,+]

[1] Department of Biomedical Sciences, University of Padova, 35131 Padova, Italy
[2] Department of Medicine, University of Cambridge, Hills Road, Cambridge CB2 0XY, UK
[3] Mitochondrial Biology Unit, University of Cambridge, Hills Road, Cambridge CB2 0XY, UK
[4] School of Chemistry, University of Glasgow, Glasgow G12 8QQ, UK
[5] Neuroscience Institute, National Research Council of Italy (CNR), 35131 Padova, Italy

[*]These authors contributed equally to this work.

[+]Joint corresponding authors:
Fabio Di Lisa, dilisa@bio.unipd.it, https://orcid.org/0000-0001-9757-8818
Thomas Krieg, tk382@medschl.cam.ac.uk, https://orcid.org/0000-0002-8900-5216

Summary

Antonucci *et al.* demonstrate that a primary increase in superoxide selectively within the mitochondria directly impacts on mitochondrial and cell function. Moreover, a slight increase in mitochondrial ROS is protective against cardiac ischaemia-reperfusion injury despite negative effects at higher concentrations.

1 <u>Abstract</u>

Reactive oxygen species (ROS) have an equivocal role in myocardial ischaemia reperfusion injury. Within the cardiomyocyte, mitochondria are both a major source and target of ROS. We evaluate the effects of a selective, dose-dependent increase in mitochondrial ROS levels on cardiac physiology using the mitochondria-targeted redox cycler MitoParaquat (MitoPQ). Low levels of ROS decrease the susceptibility of neonatal rat ventricular myocytes (NRVMs) to anoxia/reoxygenation injury and also cause profound protection in an *in vivo* mouse model of ischaemia/reperfusion. However higher doses of MitoPQ resulted in a progressive alteration of intracellular

[Ca^{2+}] homeostasis and mitochondrial function *in vitro*, leading to dysfunction and death at high doses. Our data show that a primary increase in mitochondrial ROS can alter cellular function, and support a hormetic model in which low levels of ROS are cardioprotective while higher levels of ROS are cardiotoxic.

2 Introduction

Ischaemia/reperfusion (I/R) injury occurs when the blood supply to a region of tissue is disrupted and later restored. Key to the development of the pathology is a lack of oxygen for oxidative phosphorylation within mitochondria. This results in the arrest of forward electron flow in the respiratory chain (Di Lisa et al., 1998) due to the lack of oxygen to act as the terminal electron acceptor. Consequently, succinate is accumulated during ischaemia by the reduction of fumarate at mitochondrial complex II (Chouchani et al., 2014), or from anaplerotic supply of glutamate to the tricarboxylic acid cycle leading to succinate that cannot be oxidized due to the reduced Coenzyme Q pool (Zhang et al., 2018). At reperfusion, the re-introduction of oxygen leads to sudden changes in myocardial viability, mediated by a burst of ROS production within the mitochondria. While a number of sources of ROS have been proposed to be responsible, recently it has been shown that the succinate pool accumulated during ischaemia is rapidly oxidized upon reperfusion, driving ROS production from complex I through reverse electron transport (Chouchani et al., 2014). The sustained opening of the mitochondrial permeability transition pore (mPTP), a key arbiter of cell fate, also results in significant ROS production. As ROS are among the factors contributing to prolonged mPTP opening there is a positive feedback loop of ROS-induced ROS release (Zorov et al., 2014) through which ROS generation results in sustained mitochondrial dysfunction and eventually cell death (Di Lisa et al., 2011).

However, aside from their role in driving mPTP-mediated cell damage, mitochondrial ROS production also impacts positively on several aspects of myocardial I/R injury. Mitochondrial ROS play crucial roles in signalling processes both within mitochondria and in their interplay with other cellular sites (Janssen-Heininger et al., 2008). Indeed, the protective mechanism underlying ischaemic preconditioning (IPC) appears to involve generation of low levels of ROS (Collins et al., 2012; Robin et al., 2007; Sena and Chandel, 2012). This has been demonstrated by showing that the protective effects of an IPC protocol may be abrogated by antioxidants (Eguchi et al., 2003; Hao et al., 2016; Horwitz et al., 1994; Klein et al., 1989; Mickle et al., 1989; Nishinaka et al., 1992; Peng et al., 2011), or replicated by the addition of exogenous oxidants in a pre- or post-conditioning like manner (Hegstad et al., 1997; Tritto et al., 1997; Ytrehus et al., 1995). Indeed, it has been demonstrated that the acute treatment

with H_2O_2 in a model of Langerdorff perfused hearts elicits cardioprotection in a preconditioning-like manner depending of its concentration (Valen et al., 1998; Yaguchi et al., 2003). These findings that ROS can be either cardiotoxic or cardioprotective, depending on the context, may help explain why the use of general ROS scavengers has yielded mixed results. For example there are also studies in experimental models that report no effect of antioxidants upon I/R injury (Bellows et al., 1995; Gao et al., 2002; Meyer et al., 2013; Tripathi and Hegde, 1998). In the clinic, large scale trials with antioxidants have produced equivocal effects upon cardiovascular health outcomes (Fortmann et al., 2013; Ye et al., 2013). These findings are also consistent with the growing appreciation for the differential effects of "good" and "bad" ROS (Ristow, 2014; Schwartz and Sack, 2008; Yun and Finkel, 2014), by which ROS can either contribute to cell death, or at low levels activate cardioprotective mechanisms: a concept referred to as 'hormesis'.

The context in which ROS might lead to these opposing consequences will arise due to differential effects of ROS production in three primary dimensions: in magnitude, in timing, and in spatial distribution. A better understanding of, and control of these dimensions over ROS production may provide mechanistic insights as to how ROS can have different effects. Here, we address this point by exploring the role of ROS generated within mitochondria at different concentrations, and characterize the processes linking changes in mitochondrial ROS levels to cardiac pathophysiology with focus on cardiac I/R injury. To investigate the consequences of a primary increase in ROS specifically within the mitochondrial compartment, we used the mitochondria-targeted compound MitoParaquat (MitoPQ) (Robb et al., 2015). MitoPQ was designed based upon the conjugation of a paraquat moiety (1,1'-dimethyl-4,4'-bipyridinium dichloride) (Hassan, 1984) with the mitochondria targeting triphenylphosphonium group. At the flavin site of complex I in the electron transport chain, MitoPQ accepts an electron to generate a radical monocation that reacts rapidly with oxygen to specifically generate superoxide, which is the proximal ROS species produced endogenously (Birrell et al., 2011).

In this work we demonstrate that a selective primary increase in mitochondrial ROS is a causal factor in changes of mitochondrial and cell function, and show that

low levels of mitochondrial ROS are protective against ischaemic injury both *in vitro* and *in vivo*, while higher levels are damaging.

3 <u>Results</u>

3.1 MitoPQ induces a primary increase in mitochondrial ROS levels in a dose-dependent manner

To investigate the effects of mitochondrial ROS production by MitoPQ in cardiomyocytes, neonatal rat ventricular myocytes (NRVMs) were treated for 2 h with different doses of MitoPQ. High levels of ROS were assessed with a reduced form of MitoTracker Red (MTR) that fluoresces only following oxidation. However, MTR presents some limitations due to its relative lack of sensitivity and specificity, that its accumulation depends on cell and mitochondrial membrane potential ($\Delta\Psi$m), and these can be affected by different treatments independently of ROS formation. Therefore, to detect low levels of ROS we used MitoHyPer, a genetically encoded sensor that is highly specific and sensitive for sub-micromolar concentrations of mitochondrial H_2O_2 (Belousov et al., 2006).

MitoPQ caused a significant increase in mitochondrial ROS levels in a dose-dependent manner that was not observed when cells were pre-treated with the antioxidant N-(2-Mercaptopropionyl)glycine (MPG) (**FIGURE 1A-C**). Cells treated with a MitoPQ control compound (**Supplementary FIGURE 1**) that is structurally similar to MitoPQ but which does not undergo redox cycling did not show an increase in mitochondrial ROS levels (**FIGURE 1B-D, Supplementary FIGURE 2A-B**). Moreover, cells treated with non-mitochondrial paraquat (PQ) did not show an increase in mitochondrial ROS levels (**Supplementary FIGURE 2C**), in line with previous reports (Robb et al., 2015).

Taken together, these data confirm that MitoPQ produces ROS within mitochondria in a dose-dependent manner.

3.2 A primary increase in mitochondrial ROS levels affects mitochondrial function in a dose-dependent manner

An increase in mitochondrial ROS production has been reported to induce a decrease in ΔΨm that is associated with mPTP opening (Fauconnier et al., 2007; Kokoszka et al., 2001). To investigate whether MitoPQ-induced ROS affect mitochondrial function, we monitored ΔΨm using tetramethylrhodamine fluorescence. NRVMs treated with different doses of MitoPQ displayed a dose-dependent decrease in ΔΨm (**FIGURE 2A**). Notably, although promoting H_2O_2 formation (**FIGURE 1C**), 0.01 μM MitoPQ did not affect ΔΨm. However, a defective electron transport chain may not lead to a detectable decrease in ΔΨm, since in isolated cells the proton gradient can be maintained by the reverse activity of F_OF_1 ATP synthase (Di Lisa et al., 1995). This compensatory process was abolished by the presence of the F_OF_1 ATPase inhibitor oligomycin in all the experiments. The lack of ΔΨm variations at low MitoPQ doses suggests that mild ROS formation is unlikely to alter electron transport chain function. Taken together, these results show that a primary increase in mitochondrial ROS formation decreases ΔΨm in a dose-dependent manner, but that this does not occur at low ROS levels.

Analysing the causal relationship between mPTP, ROS formation and ΔΨm is complicated by the fact that mPTP opening is both a cause and a consequence of ΔΨm loss and mitochondrial ROS generation (Bernardi, 1992; Bernardi et al., 2006; Petronilli et al., 1993). Hence, we used MitoPQ to investigate the effects of a primary increase in mitochondrial ROS levels on mPTP induction assessed by monitoring calcein fluorescence (Huser et al., 1998; Petronilli et al., 1999). NRVMs were pre-treated with or without cyclosporine A (CsA), a desensitizer of the mPTP. Since CsA is also an inhibitor of the multidrug resistance P-glycoproteins (MDR), which may alter MitoPQ distribution, cells were pre-treated also with cyclosporine H which inhibits the MDRs but does not affect mPTP opening (Dietel et al., 1994). Treatment with 0.5 μM MitoPQ induced a rapid decrease in calcein fluorescence (~30%) that was prevented by CsA. MitoPQ-induced mPTP opening was dependent on ROS formation since it was abrogated by MPG. Notably, MPG did not display any effect when mPTP opening was induced by calcimycin (**FIGURE 2B**). Taken together, these results indicate that ROS induced by 0.5 μM MitoPQ lead to mPTP opening in NRVMs.

3.3 A primary increase in mitochondrial ROS levels affects cell function and viability

We hypothesized that mitochondrial ROS would affect cellular sites and functions outside the mitochondria. In particular, our attention was focused on $[Ca^{2+}]_I$ homeostasis due to its central role in cardiac physiology (Eisner, 2014; Fearnley et al., 2011). Treatment with 0.01 µM MitoPQ caused a significant increase in both amplitude (**FIGURE 3B**) and response of the sarcoplasmic reticulum to caffeine (**FIGURE 3E**), without affecting the oscillatory pattern or the frequency of the Ca^{2+} transients (**FIGURE 3A-D**). In contrast, doses of MitoPQ > 0.01 µM induced dose-dependent alterations in all the oscillatory parameters. Notably, increasing MitoPQ concentration to 0.1 µM disrupted $[Ca^{2+}]_I$ homeostasis, causing the cells to become unexcitable (**FIGURE 3**). Overall, these findings demonstrate that ROS produced within mitochondria alter $[Ca^{2+}]_I$ homeostasis within the cytosol and endoplasmic reticulum with different amounts of ROS causing different effects.

Since oxidative stress associated with mitochondrial dysfunction is known to decrease cell viability (Carpi et al., 2009; Yancey et al., 2015), we investigated whether MitoPQ-induced oxidative stress could lead to cell death in NRVMs. The loss of cell viability was measured as lactate dehydrogenase (LDH) release in NRVMs treated for 24 h with increasing doses of MitoPQ. MitoPQ doses ≥ 0.5 µM significantly increased cell death (~30%) which could be abrogated by the addition of the free radical scavenger MPG (**FIGURE 3F**). Notably, 0.1 µM MitoPQ did not significantly alter cell viability despite promoting ROS formation, mitochondrial dysfunction and $[Ca^{2+}]_I$ dyshomeostasis without mPTP opening. Therefore, we hypothesized that the decreased cell viability at high concentrations of MitoPQ was related to mPTP opening (Bernardi et al., 2001; Di Lisa et al., 2009). This was confirmed by CsA treatment which prevented cell death induced by MitoPQ at doses ≥ 0.5 µM (**FIGURE 3G**).

3.4 Low levels of MitoPQ-induced ROS reduce cell death following anoxia/reoxygenation

We demonstrated that low doses of MitoPQ (0.01 µM) elevated ROS but did not alter mitochondrial function, $[Ca^{2+}]_I$ homeostasis and cell viability. Since an increase in mitochondrial ROS levels have been proposed to be involved in IPC (Di Lisa et al.,

2011; Halestrap, 2010; Hausenloy et al., 2016; Murphy and Steenbergen, 2007), we hypothesized that a primary increase in non-toxic mitochondrial ROS levels by MitoPQ might enhance tolerance to post-anoxic injury. To assess this, we evaluated whether the low dose of MitoPQ could mimic the protection elicited by IPC against anoxia/reoxygenation injury. Cells pre-treated with 0.01 µM MitoPQ, with or without the antioxidant MPG, were exposed to 12 h of anoxia followed by 1 h of reoxygenation. MitoPQ treatment significantly decreased cell death both at the end of anoxia and following reoxygenation. The cardioprotective effect of MitoPQ was lost in cells treated with MPG (**FIGURE 4A**). In addition, an identical concentration of the MitoPQ control compound did not induce any protection. Notably, the reliability of the protocol has been assessed by the protective effect elicited by CsA in NRVMs exposed to anoxia/reoxygenation (**Supplementary FIGURE 2D**). These data indicate that the increase in cell viability was due to MitoPQ-induced ROS.

3.5 MitoPQ reduces infarct size in an *in vivo* model of ischaemia/reperfusion injury

Finally, we utilized an *in vivo* surgical model of acute myocardial I/R injury in the mouse to determine the effect of a primary increase of ROS produced by MitoPQ upon infarct size. A bolus of MitoPQ was given by i.v. injection 15 minutes prior to the onset of cardiac ischaemia produced by occlusion of the left anterior descending coronary artery. This was followed by 2 hours reperfusion. Elevating mitochondrial ROS by intermediate doses of MitoPQ (i.e. 0.01 – 0.1 nmol) significantly reduced infarct size compared to both DMSO-only control or MitoPQ control compound (**FIGURE 4B-C-D**). However, at both lower or higher doses of MitoPQ no protection was observed, and a dose of 5 nmol MitoPQ was fatal. This shows that low levels of mitochondrial ROS can be cardioprotective during I/R injury *in vivo*, while higher levels of ROS cause damage.

Considering the changes caused in cellular calcium dynamics observed following treatment of NRVMs with MitoPQ, we evaluated its effects on haemodynamics *in vivo* using dynamic measurements of left ventricular pressure and volume. However no significant difference was observed between animals injected with the most

cardioprotective dose of MitoPQ compared with hearts treated with vehicle only (**Supplementary TABLE 1**).

4 <u>Discussion</u>

This study demonstrates that the primary formation of mitochondrial ROS exerts differential effects upon the heart during acute myocardial I/R injury, with cardioprotection conferred by a narrow intermediate dose range whilst no reduction in infarct size was observed at either higher or lower doses. This primary increase in mitochondrial ROS is also shown to have effects on mitochondrial function, $[Ca^{2+}]_I$ homeostasis and cell viability in a dose-dependent manner.

Until this point, studies assessing the effects of the alteration of intracellular ROS levels have necessarily used crude approaches to modulate ROS, which poorly mimic the (patho)physiological generation of ROS. For example, the application of exogenous hydrogen peroxide or exposure to a purine/xanthine oxygen radical generating system both require the ROS to diffuse into the cell, rather than being generated selectively within cell compartments such as the mitochondria. These limitations have been addressed by using MitoPQ (Robb et al., 2015). MitoPQ's mitochondrial accumulation allows it to be used at concentrations several hundred-fold lower than untargeted paraquat and importantly this selective accumulation means that ROS are only produced within mitochondria. The direct generation of superoxide rather than downstream ROS also mirrors its production in (patho)physiology as the proximal species (Murphy, 2009). This has been validated to occur without detectable ROS production in the cytosol (considered for publication elsewhere). The dose-dependent effect of MitoPQ on mitochondrial ROS production therefore allows the generation of exogenous ROS in a highly specific manner. Based on these features, MitoPQ represents a unique tool to investigate and characterize the effects of a precise increase in mitochondrial ROS formation on cell physiology, both *in vitro* and *in vivo*.

There is a growing body of evidence indicating that mitochondrial ROS exert differential effects depending on their dose, which has been called a "hormetic" dose-response curve (Ristow and Schmeisser, 2014). In our experiments, high levels of

ROS induced by MitoPQ (i.e. 0.5 – 1 μM) lead to mitochondrial dysfunction, mPTP opening and eventually cell death. Such detrimental effects of ROS in I/R injury through the opening of the mPTP have been well described (Di Lisa et al., 2011). Intermediate doses of ROS (i.e. 0.1 μM MitoPQ) did not affect cell viability but did cause an alteration in the amplitude of calcium transients and their response to caffeine. At low doses (i.e. 0.01 μM), ROS generation induced by MitoPQ slightly modulates $[Ca^{2+}]_I$ homeostasis without affecting either mitochondrial function or cell viability. Importantly, isolated cardiomyocytes pre-treated with low doses of MitoPQ and then exposed to anoxic injury displayed increased cell viability. This *in vitro* result was paralleled by the reduction of infarct size obtained *in vivo* in mice pre-treated with doses of MitoPQ ranging from 0.01 nmol to 1 nmol per mouse. Therefore, mitochondrial-derived ROS elicit a wide range of responses which are dependent on their dose, ranging from the disruption of $\Delta\Psi m$ and mPTP opening at high doses of MitoPQ to the reduction of cell death and infarct size at low doses of MitoPQ in a preconditioning-like manner. The absence of protective effects observed with both low and high doses of MitoPQ *in vivo* (i.e. 0.001 – 1 nmol) highlights the hormetic effect elicited by intermediate levels of ROS. Moreover, higher doses of MitoPQ (i.e. 2.5 – 5 – 10 nmol) displayed to be lethal *in vivo*. The concept of hormesis helps to rationalize the paradoxical effect of both injury and protection elicited by ROS described in literature, as well as the failure of clinical trials using general administration of antioxidants.

The data presented also show that a number of ROS-related events spread from mitochondria to the cytosolic compartment. As the source of ROS generation in our experiments is within mitochondria, we provide the first direct evidence that a primary increase in mitochondrial ROS formation can induce cardioprotection both *in vitro* and *in vivo* via changes in mitochondrial and cellular function. The known interplay between ROS and $[Ca^{2+}]_I$ homeostasis is of central relevance to the cardiomyocyte and has specifically been implicated in several disease states (Carvajal et al., 2014), but it has been difficult to determine the primacy of one factor upon the other. Taken together, our findings show that a primary increase in mitochondrial ROS can impact on the cytosol, altering $[Ca^{2+}]_I$ homeostasis and thereby whole cell function.

It is worth noting that while we have determined the doses of MitoPQ associated with the various effects in mitochondria and in intact cells, the actual concentrations of ROS required for cardiomyocytes injury and protection remain to be established due to the technically challenging nature of their measurement, especially *in vivo* (Wardman, 2007). Moreover, since we have utilised healthy young male animals for our *in vivo* model it remains to be seen how comorbidities such as obesity, diabetes, aging and sex modulate the response to a given quantity of mitochondrial ROS, since for example the protective efficacy of IPC is lost in aged or diabetic hearts (Hausenloy et al., 2016).

In conclusion, we have demonstrated that a primary increase in mitochondrial ROS exerts effects on both mitochondrial and cell function, which presents mitochondrial ROS as a cause rather than consequence of the functional change in cardiac (patho)physiology. Notably, the generation of exogenous ROS by MitoPQ within mitochondria is found to exert differential effects, with a hormetic dose response curve in which protection is observed only at an intermediate level of mitochondrial ROS, but not at either lower or higher levels.

5 Methods

5.1 Cell culture

5.1.1 NRVMs

Neonatal rat ventricular myocytes (NRVMs) were isolated from 1-3 day old Wistar rats as described previously (Kaludercic et al., 2014). Briefly, hearts were excised, cut into smaller pieces and left overnight at 4°C for digestion by 2.5% trypsin 10X (Thermo Fisher Scientific) in HBSS (Sigma). The next day, tissues were incubated with 0.75 mg/ml collagenase type II (Thermo Fisher Scientific) in HBSS for 10 min (at 2 min intervals) at 37°C and cells dissociated by pipetting. Following centrifugation at 300 g for 7 min, cells were resuspended in MEM (Invitrogen) and pre-plated for 2 h to let cardiac fibroblasts attach to the plastic surface. Plates and coverslips were coated with a solution of 0.1% porcine gelatin (Sigma) and incubated at 37°C for 1 h. The

non-adherent myocytes were plated in gelatin coated plates at variable density (at least 1×10^5 cells/ml) in MEM supplemented with 10% FBS (Thermo Fisher Scientific), 1% penicillin/streptomycin (Thermo Fisher Scientific), 1% non-essential amino acids (Thermo Fisher Scientific), 1 mM 5-Bromo-2-Deoxyuridine (Sigma). Cells were maintained at 37°C in presence of 5% CO_2. The medium was changed to MEM supplemented with 1% FBS, 1% penicillin/streptomycin and 1% non-essential amino acids after 24 h of plating.

To evoke a primary increase in mitochondrial ROS, NRVMs were treated in culture medium with different concentrations of MitoPQ (Robb et al., 2015), from 0.01 to 1 µM for 2 h, unless specified in results. A MitoPQ control compound was also used that has a very similar structure to MitoPQ and similar levels of uptake into mitochondria, but which cannot generate ROS by redox cycling. MitoPQ redox cycles because it can receive an electron from the $FMNH_2$ of complex I reducing the viologen dication to a radical cation, which then reduces oxygen to superoxide to regenerate MitoPQ (**Supplemental FIGURE 1**). MitoPQ control employs the twisted viologen unit described by (Andersson et al., 2009), in which two extra methyl groups disfavour the coplanarity of the two pyridine units required to stabilize a radical cation. We have previously reported its use (Fazakerley et al., 2018), but here give full details of its synthesis in two steps by double alkylation of 3'-dimethyl-4,4'-dipyridyl, prepared by the procedure of (Rebek et al., 1985) (**Supplementary FIGURE 3**). To scavenge ROS, cells were pre-treated with 500 µM MPG (Sigma) (Perrelli et al., 2011) for 30 min. To prevent mPTP opening, cells were pre-treated with 1 µM CsA (Sigma) (Di Lisa et al., 2001) for 30 min.

5.1.2 Transfection

NRVMs were plated on six-well plates at a density of 3×10^5 cells/well and transfected with Lipofectamine 3000 reagent (Sigma). For each transfection, 2.5 µg of MitoHyPer (Evrogen) was diluted in 125 µl of Opti-MEM medium (Thermo Fisher Scientific) in presence of 5 µl of P3000™ reagent (Life Technologies) and later combined with 4 µl of Lipofectamine™ 3000 (Life Technologies). The DNA-lipid complexes were added to the cells and incubated overnight. The day after, cells were rinsed with PBS and new MEM was added. Transfected cells were used for experiments after 48 h.

5.1.3 Imaging

Experiments using NRVMs were carried out in HBSS at pH 7.4 (adjusted with NaOH) and at 37 °C.

Images were acquired using an inverted fluorescence microscope (Leica DMI6000B equipped with DFC365FX camera) with PL APO 40x/1.25 oil objective. Fluorescence intensity was quantified using the Fiji distribution of the Java-based image processing program ImageJ (Schindelin et al., 2012), and background signal was subtracted from all analysed regions of interest. For Ca^{2+} imaging, traces were analysed using the "Peak Analyzer" tool of Origin Pro 9.1.

To monitor mitochondrial ROS formation, cells were incubated with 25 nM MitoTracker Red CM-H_2XRos (MTR, Thermo Fisher Scientific) for 30 min at 37°C in a humidified incubator. Since the accumulation of MTR in NRVMs can vary from different preparation, data were normalized to DMSO control.

To monitor mitochondrial membrane potential (ΔΨm), cells were incubated with 25 nM tetramethylrhodamine (TMRM, Thermo Fisher Scientific) in presence of 1.6 μM cyclosporin H (CsH) for 30 min at 37°C in a humidified incubator. TMRM fluorescence intensity was monitored following addition of 4 μM oligomycin (Sigma) and images were acquired before and after the addition of 4 μM carbonyl cyanide-p-trifluoromethoxyphenylhydrazone (FCCP, Sigma) (Kaludercic et al., 2014). In order to have a reliable value of TMRM, fluorescence values were expressed as ΔF (F_0/F_{FCCP}) and results were normalized to DMSO control basal value.

To monitor mPTP opening, cells were incubated with 1 μM calcein acetoxymethyl (AM) ester (Thermo Fisher Scientific) in presence of 1 mM Cobalt Chloride ($CoCl_2$) for 15 min at 37°C in a humidified incubator as previously described (Petronilli et al., 1999). To evaluate the extent of pore opening, data were normalized to the basal value.

To monitor [Ca^{2+}]$_i$ homeostasis, cells were incubated with 5 μM Fluo-4 AM ester (Thermo Fisher Scientific), 0.01% w/v pluronic F-127 (Sigma) and 250 μM sulfinpyrazone (Sigma), for 20 min at 37°C in MEM followed by 20 min of de-

esterification. Since the accumulation of Fluo-4 in NRVMs can vary from different preparation, data were normalized to DMSO control.

5.1.4 Assessment of cell death

For normoxic experiments, NRVMs were seeded in 24w plates at density of 10^5 cells/well and cultured in MEM supplemented with 1% FBS, 1% penicillin/streptomycin and 1% non-essential amino acids. Cells were incubated with different concentrations of MitoPQ with or without MPG or CsA for 24 h at 37°C in a humidified incubator

For anoxia/reperfusion experiments, NRVMs were seeded in 24w plates at density of 10^5 cells/well and incubated in 118 mM NaCl, 5 mM KCl, 1.2 mM KH_2PO_4, 1.2 mM $MgSO_4$, 2 mM $CaCl_2$, 25 mM MOPS at pH 6.4 during anoxia or pH 7.4 during reoxygenation (Bond et al., 1991). Anoxia was induced adding 10 mM 2-deoxy-D-glucose (2-DG) and incubating in a BD GasPak™ EZ Anaerobe Gas-generating Pouch System with an indicator (BD Biosciences) at 37°C for 12 h (Matsuoka et al., 2002). To induce reoxygenation, plates were removed from the GasPak™ pouch, 2-DG was replaced with 10 mM D-glucose, the pH was restored at 7.4. The plates were then incubated for 1 h in a humidified incubator at 37°C.

The release of LDH from NRVMs was measured to evaluate cell death occurring in normoxia, anoxia and reoxygenation as described before (Bergmeyer and Bernt, 1974; Di Lisa et al., 2001). Supernatant aliquots were collected after 24 h of normoxia, 12 h of anoxia and 1 h of reoxygenation. At the end of every experiment, intact cells were lysed by incubating with 1% Triton X-100 (Sigma) for 30 min and supernatants were collected to evaluate the total amount of LDH. LDH enzymatic activity was measured spectrophotometrically by the absorbance of nicotinamide adenine dinucleotide (Roche) at 340 nm, indicative of the reduction of pyruvate to lactate.

5.2 Experimental Animals

Male C57BL/6J mice aged 8-10 weeks (22-32 g) were obtained from Charles River, UK. They were housed under standard laboratory conditions, with food and water available *ad libitum*. All procedures were carried out in accordance with the UK Home Office Guide on the Operation of Animal (Scientific Procedures) Act 1986 and

University of Cambridge Animal Welfare Policy under project licenses 70/8238 and 70/7963.

5.3 Open-chest mouse model of acute myocardial I/R Injury

An open chest model of acute myocardial ischaemia/reperfusion injury was used as described elsewhere (Eckle et al., 2006). Mice were anesthetized with sodium pentobarbital (70 mg/kg intraperitoneal), with depth of anaesthesia monitored via the pedal reflex and additional anaesthesia administered as required. Following left side lateral thoracotomy, the left anterior descending coronary artery was occluded for 30 min followed by 2 h of reperfusion. Compounds were administered 15 min prior to the start of ischaemia by an intravenous bolus injection in the lateral tail vein.

At the end of the protocol, the area at risk was delineated by retrograde injection of 10 mg/ml Evans Blue after re-occlusion of the left anterior descending coronary artery. Heart sections were incubated for 25 min at 37°C in 1% triphenyltetrazolium chloride (Sigma, UK) before fixing for 24 h in 10% formalin. Planimetry was performed in a blinded fashion using ImageJ (Schneider et al., 2012). Hearts in which the area at risk was outside of the range 30% - 60% of total area were excluded from any further analysis.

5.4 Pressure-Volume analysis of cardiac function

Anaesthesia was induced with 3% isoflurane in O_2 in a plexiglass chamber. Mice were transferred to a heated surgical platform, and sufficient isoflurane administered to maintain a surgical plane of anaesthesia as assessed by the pedal reflex. Body temperature was maintained at 37°C using a rectal thermometer and temperature controller (TCAT-2LV, Physitemp, USA). The left ventricle was catheterized via the right carotid artery with a 1.2 French tetrapolar catheter (Transonic Scisense Inc, Canada) as described elsewhere (Pacher et al., 2008). In brief, a small midline incision was made in the neck in order to expose the carotid artery and isolate it from the vagus nerve. A 4-0 silk suture was tied tightly around the distal end of the artery, and two more sutures were placed loosely at the proximal end. Using a vascular clamp (0.4-1 mm) to minimize blood loss, a small incision was made in the carotid artery with microscissors and the catheter inserted and secured using the additional sutures. The

catheter was the inserted along the carotid until it was located centrally within the left ventricle, as indicated by the phase signal and by the shape of the resultant pressure-magnitude loops. At least 15 min were allowed for the haemodynamics to stabilize. A 100 μL bolus containing either 0.1 nmol MitoPQ or vehicle only was then injected via the lateral tail vein. Data were recorded at 1000 Hz using the ADV500 PV system (Transonic Scisense Inc, Canada) and a multi-channel acquisition system (Powerlab, ADInstruments, UK) and were analysed in LabChart (ADInstruments, UK). Volumes were calculated on dynamic basis using Wei's equation (Larson et al., 2013). Three short sections of loops (within one breathing cycle) were examined at both baseline conditions and >5 minutes following injection. Upon completion of the protocol all animals were killed via cervical dislocation.

5.5 Chemical synthesis

MitoPQ was synthesized from iododecyl-TPP salt **1**, which was prepared as described previously (Robb et al.) (**Supplementary FIGURE 3**). This was reacted with an excess of dimethyl-4,4'-dipyridyl **2**, prepared by the procedure of (Rebek et al.), to minimise dialkylation. The monoalkylated product **3** was isolated in excellent year and was then methylated to give complete conversion to MitoPQ control.

5.5.1 3-Methyl-4-(3"-methylpyrid-4"-yl)-1-(10"'-triphenylphosphoniodec-1"'-yl)pyridinium diiodide 3

(10-Iododec-1-yl)triphenylphosphonium iodide **1** (107 mg, 0.163 mmol, 1.0 eq.) was added to a solution of 3,3'-Dimethyl-4,4'-dipyridyl **2** (120 mg, 0.65 mmol, 4.0 eq) in MeCN (2 ml) and the resulting solution was heated to 60°C overnight under an atmosphere of argon. The solution was cooled to RT and concentrated under vacuum. Column chromatography eluting with CH_2Cl_2-MeOH (100:0 to 85:15) then gave the pyridinium salt **3** as an off-white solid (116 mg, 85%). ν_{max} (ATR): 2926 (CH), 2854 (CH), 1635 (Ar), 1437 (CH) cm^{-1}. δ_H (400 MHz, CDCl$_3$): 9.98 (1H, s, H-1), 9.71 (1H, d, J = 6.3 Hz, H-2), 8.62 (1H, s, H-4), 8.58 (1H, d, J = 5.0 Hz, H-5), 7.86-7.68 (16H, m, PPh$_3$ + H-3), 7.06 (1H, d, J = 4.9 Hz, H-6), 4.97 (2H, t, J = 7.8 Hz, NCH$_2$), 3.61-3.51 (2H, m, PCH$_2$), 2.37 (3H, s, CH$_3$), 2.32 – 2.16 (2H, m, NCH$_2$CH$_2$), 2.10 (3H, s, CH$_3$), 1.70-1.60 (8H, m, 4 × CH$_2$), 1.59-1.50 (2H, m, CH$_2$), 1.49-1.25 (4H, m, 2 × CH$_2$). δ_C (101 MHz, CDCl$_3$): 154.85 (C), 151.42 (CH), 147.46 (CH), 145.16 (CH), 142.50 (CH),

137.03 (C), 134.94 (d, J = 3.0 Hz, CH), 133.25 (d, J = 10.0 Hz, CH), 130.32 (d, J = 12.6 Hz, CH), 129.32 (C), 127.45 (CH), 121.39 (CH), 117.60 (d, J = 86.0 Hz, C), 60.75 (CH_2), 31.17 (CH_2), 29.81 (d, J = 15.8 Hz, CH_2), 28.26 (CH_2) , 28.17 (CH_2), 27.99 (CH_2), 27.96 (CH_2), 25.41 (CH_2), 22.70 (d, J = 50.4 Hz, CH_2), 22.11 (d, J = 4.4 Hz, CH_2), 16.81 (CH_3), 16.48 (CH_3). δ_P (162 MHz: $CDCl_3$): 23.94 (s). m/z (ESI): Found: 293.1734. $C_{40}H_{47}N_2P$ requires (M^{2+}), 293.1733.

5.5.2 1,3,3'-trimethyl-1'-(10"'-triphenylphosphoniodec-1"'-yl)-4,4'-bipyridinium (MitoPQ control) triiodide

Iodomethane (19 µL, 0.29 mmol, 5.0 eq.) was added to a solution of pyridine **3** (49 mg, 0.058mmol, 1.0 eq) in MeCN (1 ml) and the resulting solution was heated to 40°C overnight under an atmosphere of argon. The solution was cooled to RT and concentrated under vacuum to give the MitoPQ triiodide as an off-white solid (57 mg, 100%). ν_{max} (ATR): 3016 (CH), 2926 (CH), 2854 (CH), 1635 (Ar), 1437 (CH) cm^{-1}. δ_H (400 MHz, d3-MeCN): 9.14 (1H, s, H-1), 8.94 (1H, s, H-4), 8.91 (1H, d, J = 6.3 Hz, H-2), 8.77 (1H, d, J = 6.3 Hz, H-5), 7.99 – 7.86 (5H, m, H-3, H-6 + 3 × ArH), 7.81 – 7.71 (12H, m, 12 × ArH), 4.67 (2H, t, J = 7.6 Hz, NCH_2), 4.42 (3H, s, NCH_3), 3.35-3.23 (2H, m, PCH_2), 2.30 (3H, s, CH_3), 2.29 (3H, s, CH_3), 2.07 (2H, q, J = 7.3 Hz, NCH_2CH_2), 1.70-1.60 (2H, m, PCH_2CH_2), 1.58-1.49 (2H, m, CH_2), 1.47-1.25 (10H, m, 5 × CH_2). δ_C (101 MHz, d3-MeCN): 152.15 (C), 147.69 (CH), 146.81 (CH), 143.92 (CH), 143.12 (CH), 138.41 (C), 137.98 (C), 135.86 (d, J = 3.0 Hz, CH), 134.55 (d, J = 10.0 Hz, CH), 130.07 (d, J = 12.5 Hz, CH), 128.04 (CH), 127.81 (CH), 119.31 (d, J = 86.2 Hz, C), 62.20 (CH_2), 49.19 (CH_3), 31.74 (CH_2), 30.76 (d, J = 16.2 Hz, CH_2), 29.55 (CH_2), 29.48 (CH_2), 29.30 (CH_2), 29.04 (CH_2), 26.35 (CH_2), 22.81 (d, J = 4.4 Hz, CH_2), 22.61 (d, J = 50.7 Hz, CH_2), 17.54 (CH_3), 17.41 (CH_3). δ_P (162 MHz: d3-MeCN): 23.84 (s). m/z (ESI): Found: 200.4568. $C_{41}H_{50}N_2P$ requires (M^{3+}), 200.4565.

5.6 Data analysis

All values are expressed as mean ± S.E.M. Every set of data has 3 biological replicates (i.e. 3 different cardiac preparations) and every biological replicate has at least 3 technical replicates (i.e. 3 different samples of the same preparation). The propagation of error analysis was performed to take into account the uncertainty that is present in the experimental measurements due to measurement limitations (i.e.

different accumulation of the sensor in NRVMs derived from different preparations). Comparison between groups was performed by one-way ANOVA, followed by post hoc testing (i.e. Tukey's range test, Dunnett's test) adjusted for multiple comparisons where data were normally distributed. Data that did not follow the normal distribution were statistically analysed by Kolgomorov-Smirnov's test. Comparison between two groups was performed using a two-tailed Student's t-test, with correction for multiple testing by the Bonferroni method where appropriate. A value of $p < 0.05$ was considered significant.

6 <u>Acknowledgements</u>

7 <u>Abbreviations</u>

$[Ca^{2+}]_I$ – intracellular calcium concentration
A/R – anoxia/reoxygenation
CsA - cyclosporine A
IPC – ischaemic preconditioning
I/R – ischaemia/reperfusion
LDH – lactate dehydrogenase
MitoPQ – MitoParaquat
MPG - N-(2-Mercaptopropionyl)glycine
mPTP – Mitochondrial permeability transition pore
MTR – mitotracker red CMH_2X-ROS
NRVM – neonatal rat ventricular myocytes
TMRM - tetramethylrhodamine
ΔΨm - mitochondrial membrane potential

8   <u>References</u>

Andersson S., D.P. Zou, R. Zhang, S.G. Sun, B. Akermark and L.C. Sun. 2009. Selective Positioning of CB 8 on Two Linked Viologens and Electrochemically Driven Movement of the Host Molecule. *European Journal of Organic Chemistry*:1163-1172.

Bellows, S.D., S.L. Hale, B.Z. Simkhovich, G.L. Kay, and R.A. Kloner. 1995. Do antioxidant vitamins reduce infarct size following acute myocardial ischemia/reperfusion? *Cardiovascular drugs and therapy* 9:117-123.

Belousov, V.V., A.F. Fradkov, K.A. Lukyanov, D.B. Staroverov, K.S. Shakhbazov, A.V. Terskikh, and S. Lukyanov. 2006. Genetically encoded fluorescent indicator for intracellular hydrogen peroxide. *Nature methods* 3:281-286.

Bergmeyer, H.U., and E. Bernt. 1974. Methods of Enzymatic Analysis. Verlag Chemie, Weinheim, Germany. 607-612 pp.

Bernardi, P. 1992. Modulation of the mitochondrial cyclosporin A-sensitive permeability transition pore by the proton electrochemical gradient. Evidence that the pore can be opened by membrane depolarization. *The Journal of biological chemistry* 267:8834-8839.

Bernardi, P., A. Krauskopf, E. Basso, V. Petronilli, E. Blachly-Dyson, F. Di Lisa, and M.A. Forte. 2006. The mitochondrial permeability transition from in vitro artifact to disease target. *The FEBS journal* 273:2077-2099.

Bernardi, P., V. Petronilli, F. Di Lisa, and M. Forte. 2001. A mitochondrial perspective on cell death. *Trends in biochemical sciences* 26:112-117.

Birrell, J.A., M.S. King, and J. Hirst. 2011. A ternary mechanism for NADH oxidation by positively charged electron acceptors, catalyzed at the flavin site in respiratory complex I. *FEBS letters* 585:2318-2322.

Bond, J.M., B. Herman, and J.J. Lemasters. 1991. Protection by acidic pH against anoxia/reoxygenation injury to rat neonatal cardiac myocytes. *Biochemical and biophysical research communications* 179:798-803.

Carpi, A., R. Menabo, N. Kaludercic, P. Pelicci, F. Di Lisa, and M. Giorgio. 2009. The cardioprotective effects elicited by p66(Shc) ablation demonstrate the crucial role of mitochondrial ROS formation in ischemia/reperfusion injury. *Biochimica et biophysica acta* 1787:774-780.

Carvajal, K., J. Balderas-Villalobos, M.D. Bello-Sanchez, B. Phillips-Farfan, T. Molina-Munoz, H. Aldana-Quintero, and N.L. Gomez-Viquez. 2014. Ca(2+) mishandling and cardiac dysfunction in obesity and insulin resistance: role of oxidative stress. *Cell calcium* 56:408-415.

Chouchani, E.T., V.R. Pell, E. Gaude, D. Aksentijevic, S.Y. Sundier, E.L. Robb, A. Logan, S.M. Nadtochiy, E.N.J. Ord, A.C. Smith, F. Eyassu, R. Shirley, C.H. Hu, A.J. Dare, A.M. James, S. Rogatti, R.C. Hartley, S. Eaton, A.S.H. Costa, P.S. Brookes, S.M. Davidson, M.R. Duchen, K. Saeb-Parsy, M.J. Shattock, A.J. Robinson, L.M. Work, C. Frezza, T. Krieg, and M.P. Murphy. 2014. Ischaemic accumulation of succinate controls reperfusion injury through mitochondrial ROS. *Nature* 515:431-435.

Collins, Y., E.T. Chouchani, A.M. James, K.E. Menger, H.M. Cocheme, and M.P. Murphy. 2012. Mitochondrial redox signalling at a glance. *Journal of cell science* 125:801-806.

Di Lisa, F., P.S. Blank, R. Colonna, G. Gambassi, H.S. Silverman, M.D. Stern, and R.G. Hansford. 1995. Mitochondrial membrane potential in single living adult rat cardiac myocytes exposed to anoxia or metabolic inhibition. *J Physio* 1-13.

Di Lisa, F., M. Canton, A. Carpi, N. Kaludercic, R. Menabo, S. Menazza, and M. Semenzato. 2011. Mitochondrial injury and protection in ischemic pre- and postconditioning. *Antioxidants & redox signaling* 14:881-891.

Di Lisa, F., N. Kaludercic, A. Carpi, R. Menabo, and M. Giorgio. 2009. Mitochondria and vascular pathology. *Pharmacological reports : PR* 61:123-130.

Di Lisa, F., R. Menabo, M. Canton, M. Barile, and P. Bernardi. 2001. Opening of the mitochondrial permeability transition pore causes depletion of mitochondrial and cytosolic NAD+ and is a causative event in the death of myocytes in postischemic reperfusion of the heart. *The Journal of biological chemistry* 276:2571-2575.

Di Lisa, F., R. Menabo, M. Canton, and V. Petronilli. 1998. The role of mitochondria in the salvage and the injury of the ischemic myocardium. *Biochimica et biophysica acta* 1366:69-78.

Dietel, M., I. Herzig, A. Reymann, I. Brandt, B. Schaefer, A. Bunge, H.J. Heidebrecht, and A. Seidel. 1994. Secondary combined resistance to the multidrug-resistance-reversing activity of cyclosporin A in the cell line F4-6RADR-CsA. *Journal of cancer research and clinical oncology* 120:263-271.

Eckle, T., A. Grenz, D. Kohler, A. Redel, M. Falk, B. Rolauffs, H. Osswald, F. Kehl, and H.K. Eltzschig. 2006. Systematic evaluation of a novel model for cardiac ischemic preconditioning in mice. *American journal of physiology. Heart and circulatory physiology* 291:H2533-2540.

Eguchi, M., M. Fujiwara, Y. Mizukami, and N. Miwa. 2003. Cytoprotection by pro-vitamin C against ischemic injuries in perfused rat heart together with differential activation of MAP kinase family. *Journal of cellular biochemistry* 89:863-867.

Eisner, D. 2014. Calcium in the heart: from physiology to disease. *Experimental physiology* 99:1273-1282.

Fauconnier, J., D.C. Andersson, S.J. Zhang, J.T. Lanner, R. Wibom, A. Katz, J.D. Bruton, and H. Westerblad. 2007. Effects of palmitate on Ca(2+) handling in adult control and ob/ob cardiomyocytes: impact of mitochondrial reactive oxygen species. *Diabetes* 56:1136-1142.

Fazakerley, D.J., A.Y. Minard, J.R. Krycer, K.C. Thomas, J. Stockli, D.J. Harney, J.G. Burchfield, G.J. Maghzal, S.T. Caldwell, R.C. Hartley, R. Stocker, M.P. Murphy, and D.E. James. 2018. Mitochondrial oxidative stress causes insulin resistance without disrupting oxidative phosphorylation. *The Journal of biological chemistry* 293:7315-7328.

Fearnley, C.J., H.L. Roderick, and M.D. Bootman. 2011. Calcium signaling in cardiac myocytes. *Cold Spring Harbor perspectives in biology* 3:a004242.

Fortmann, S.P., B.U. Burda, C.A. Senger, J.S. Lin, and E.P. Whitlock. 2013. Vitamin and mineral supplements in the primary prevention of cardiovascular disease and cancer: An updated systematic evidence review for the U.S. Preventive Services Task Force. *Annals of internal medicine* 159:824-834.

Gao, F., C.L. Yao, E. Gao, Q.Z. Mo, W.L. Yan, R. McLaughlin, B.L. Lopez, T.A. Christopher, and X.L. Ma. 2002. Enhancement of glutathione cardioprotection by ascorbic acid in myocardial reperfusion injury. *The Journal of pharmacology and experimental therapeutics* 301:543-550.

Halestrap, A.P. 2010. A pore way to die: the role of mitochondria in reperfusion injury and cardioprotection. *Biochemical Society transactions* 38:841-860.

Hao, J., W.W. Li, H. Du, Z.F. Zhao, F. Liu, J.C. Lu, X.C. Yang, and W. Cui. 2016. Role of Vitamin C in Cardioprotection of Ischemia/Reperfusion Injury by Activation of Mitochondrial KATP Channel. *Chemical & pharmaceutical bulletin* 64:548-557.

Hassan, H.M. 1984. Exacerbation of superoxide radical formation by paraquat. *Methods in enzymology* 105:523-532.

Hausenloy, D.J., J.A. Barrabes, H.E. Botker, S.M. Davidson, F. Di Lisa, J. Downey, T. Engstrom, P. Ferdinandy, H.A. Carbrera-Fuentes, G. Heusch, B. Ibanez, E.K. Iliodromitis, J. Inserte, R. Jennings, N. Kalia, R. Kharbanda, S. Lecour, M. Marber, T. Miura, M. Ovize, M.A. Perez-Pinzon, H.M. Piper, K. Przyklenk, M.R. Schmidt, A. Redington, M. Ruiz-Meana, G. Vilahur, J. Vinten-Johansen, D.M. Yellon, and D. Garcia-Dorado. 2016. Ischaemic conditioning and targeting reperfusion injury: a 30 year voyage of discovery. *Basic research in cardiology* 111:70.

Hegstad, A.C., O.H. Antonsen, and K. Ytrehus. 1997. Low concentrations of hydrogen peroxide improve post-ischaemic metabolic and functional recovery in isolated perfused rat hearts. *Journal of molecular and cellular cardiology* 29:2779-2787.

Horwitz, L.D., P.V. Fennessey, R.H. Shikes, and Y. Kong. 1994. Marked reduction in myocardial infarct size due to prolonged infusion of an antioxidant during reperfusion. *Circulation* 89:1792-1801.

Huser, J., C.E. Rechenmacher, and L.A. Blatter. 1998. Imaging the permeability pore transition in single mitochondria. *Biophysical journal* 74:2129-2137.

Janssen-Heininger, Y.M., B.T. Mossman, N.H. Heintz, H.J. Forman, B. Kalyanaraman, T. Finkel, J.S. Stamler, S.G. Rhee, and A. van der Vliet. 2008. Redox-based regulation of signal transduction: principles, pitfalls, and promises. *Free radical biology & medicine* 45:1-17.

Kaludercic, N., A. Carpi, T. Nagayama, V. Sivakumaran, G. Zhu, E.W. Lai, D. Bedja, A. De Mario, K. Chen, K.L. Gabrielson, M.L. Lindsey, K. Pacak, E. Takimoto, J.C. Shih, D.A. Kass, F. Di Lisa, and N. Paolocci. 2014. Monoamine oxidase B prompts mitochondrial and cardiac dysfunction in pressure overloaded hearts. *Antioxidants & redox signaling* 20:267-280.

Klein, H.H., S. Pich, S. Lindert, K. Nebendahl, P. Niedmann, and H. Kreuzer. 1989. Combined treatment with vitamins E and C in experimental myocardial infarction in pigs. *American heart journal* 118:667-673.

Kokoszka, J., P. Coskun, L. Esposito, and D. Wallace. 2001. Increased mitochondrial oxidative stress in the Sod2 (+/-) mouse results in the age-related decline of mitochondrial function culminating in increased apoptosis. *Proceedings of the National Academy of Sciences of the United States of America* 98:2278-2283.

Matsuoka, R., K. Ogawa, H. Yaoita, W. Naganuma, K. Maehara, and Y. Maruyama. 2002. Characteristics of death of neonatal rat cardiomyocytes following hypoxia or hypoxia-reoxygenation: the association of apoptosis and cell membrane disintegrity. *Heart and vessels* 16:241-248.

Meyer, M., S.P. Bell, Z. Chen, I. Nyotowidjojo, R.R. Lachapelle, T.F. Christian, P.C. Gibson, F.F. Keating, H.L. Dauerman, and M.M. LeWinter. 2013. High dose intracoronary N-acetylcysteine in a porcine model of ST-elevation myocardial infarction. *Journal of thrombosis and thrombolysis* 36:433-441.

Mickle, D.A., R.K. Li, R.D. Weisel, P.L. Birnbaum, T.W. Wu, G. Jackowski, M.M. Madonik, G.W. Burton, and K.U. Ingold. 1989. Myocardial salvage with trolox and ascorbic acid for an acute evolving infarction. *The Annals of thoracic surgery* 47:553-557.

Murphy, E., and C. Steenbergen. 2007. Preconditioning: the mitochondrial connection. *Annual review of physiology* 69:51-67.

Murphy, M.P. 2009. How mitochondria produce reactive oxygen species. *The Biochemical journal* 417:1-13.

Nishinaka, Y., S. Sugiyama, M. Yokota, H. Saito, and T. Ozawa. 1992. The effects of a high dose of ascorbate on ischemia-reperfusion-induced mitochondrial dysfunction in canine hearts. *Heart and vessels* 7:18-23.

Peng, Y.W., C.L. Buller, and J.R. Charpie. 2011. Impact of N-acetylcysteine on neonatal cardiomyocyte ischemia-reperfusion injury. *Pediatric research* 70:61-66.

Perrelli, M.G., P. Pagliaro, and C. Penna. 2011. Ischemia/reperfusion injury and cardioprotective mechanisms: Role of mitochondria and reactive oxygen species. *World journal of cardiology* 3:186-200.

Petronilli, V., C. Cola, S. Massari, R. Colonna, and P. Bernardi. 1993. Physiological effectors modify voltage sensing by the cyclosporin A-sensitive permeability transition pore of mitochondria. *The Journal of biological chemistry* 268:21939-21945.

Petronilli, V., G. Miotto, M. Canton, M. Brini, R. Colonna, P. Bernardi, and F. Di Lisa. 1999. Transient and long-lasting openings of the mitochondrial permeability transition pore can be monitored directly in intact cells by changes in mitochondrial calcein fluorescence. *Biophysical journal* 76:725-734.

Ristow, M. 2014. Unraveling the truth about antioxidants: mitohormesis explains ROS-induced health benefits. *Nature medicine* 20:709-711.

Ristow, M., and K. Schmeisser. 2014. Mitohormesis: Promoting Health and Lifespan by Increased Levels of Reactive Oxygen Species (ROS). *Dose-response : a publication of International Hormesis Society* 12:288-341.

Robb, E.L., J.M. Gawel, D. Aksentijevic, H.M. Cocheme, T.S. Stewart, M.M. Shchepinova, H. Qiang, T.A. Prime, T.P. Bright, A.M. James, M.J. Shattock, H.M. Senn, R.C. Hartley, and M.P. Murphy. 2015. Selective superoxide generation within mitochondria by the targeted redox cycler MitoParaquat. *Free radical biology & medicine* 89:883-894.

Robin, E., R.D. Guzy, G. Loor, H. Iwase, G.B. Waypa, J.D. Marks, T.L. Hoek, and P.T. Schumacker. 2007. Oxidant stress during simulated ischemia primes cardiomyocytes for cell death during reperfusion. *The Journal of biological chemistry* 282:19133-19143.

Schindelin, J., I. Arganda-Carreras, E. Frise, V. Kaynig, M. Longair, T. Pietzsch, S. Preibisch, C. Rueden, S. Saalfeld, B. Schmid, J.Y. Tinevez, D.J. White, V. Hartenstein, K. Eliceiri, P. Tomancak, and A. Cardona. 2012. Fiji: an open-source platform for biological-image analysis. *Nature methods* 9:676-682.

Schneider, C.A., W.S. Rasband, and K.W. Eliceiri. 2012. NIH Image to ImageJ: 25 years of image analysis. *Nature methods* 9:671-675.

Schwartz, D.R., and M.N. Sack. 2008. Targeting the mitochondria to augment myocardial protection. *Current opinion in pharmacology* 8:160-165.

Sena, L.A., and N.S. Chandel. 2012. Physiological roles of mitochondrial reactive oxygen species. *Molecular cell* 48:158-167.

Tripathi, Y., and B.M. Hegde. 1998. Effect of N-acetylcysteine on myocardial infarct size following ischemia and reperfusion in dogs. *Indian journal of physiology and pharmacology* 42:50-56.

Tritto, I., D. D'Andrea, N. Eramo, A. Scognamiglio, C. De Simone, A. Violante, A. Esposito, M. Chiariello, and G. Ambrosio. 1997. Oxygen radicals can induce preconditioning in rabbit hearts. *Circulation research* 80:743-748.

Valen, G., J. Starkopf, S. Takeshima, T. Kullisaar, T. Vihalemm, A.T. Kengsepp, C. Lowbeer, J. Vaage, and M. Zilmer. 1998. Preconditioning with hydrogen peroxide (H2O2) or ischemia in H2O2-induced cardiac dysfunction. *Free radical research* 29:235-245.

Wardman, P. 2007. Fluorescent and luminescent probes for measurement of oxidative and nitrosative species in cells and tissues: progress, pitfalls, and prospects. *Free radical biology & medicine* 43:995-1022.

Yaguchi, Y., H. Satoh, N. Wakahara, H. Katoh, A. Uehara, H. Terada, Y. Fujise, and H. Hayashi. 2003. Protective effects of hydrogen peroxide against ischemia/reperfusion injury in perfused rat hearts. *Circulation journal : official journal of the Japanese Circulation Society* 67:253-258.

Yancey, D.M., J.L. Guichard, M.I. Ahmed, L. Zhou, M.P. Murphy, M.S. Johnson, G.A. Benavides, J. Collawn, V. Darley-Usmar, and L.J. Dell'Italia. 2015. Cardiomyocyte mitochondrial oxidative stress and cytoskeletal breakdown in the heart with a primary volume overload. *American journal of physiology. Heart and circulatory physiology* 308:H651-663.

Ye, Y., J. Li, and Z. Yuan. 2013. Effect of antioxidant vitamin supplementation on cardiovascular outcomes: a meta-analysis of randomized controlled trials. *PloS one* 8:e56803.

Ytrehus, K., R.S. Walsh, S.C. Richards, and J.M. Downey. 1995. Hydrogen peroxide as a protective agent during reperfusion. A study in the isolated perfused rabbit heart subjected to regional ischemia. *Cardiovascular research* 30:1033-1037.

Yun, J., and T. Finkel. 2014. Mitohormesis. *Cell metabolism* 19:757-766.

Zhang, J., Y.T. Wang, J.H. Miller, M.M. Day, J.C. Munger, and P.S. Brookes. 2018. Accumulation of Succinate in Cardiac Ischemia Primarily Occurs via Canonical Krebs Cycle Activity. *Cell reports* 23:2617-2628.

Zorov, D.B., M. Juhaszova, and S.J. Sollott. 2014. Mitochondrial reactive oxygen species (ROS) and ROS-induced ROS release. *Physiological reviews* 94:909-950.
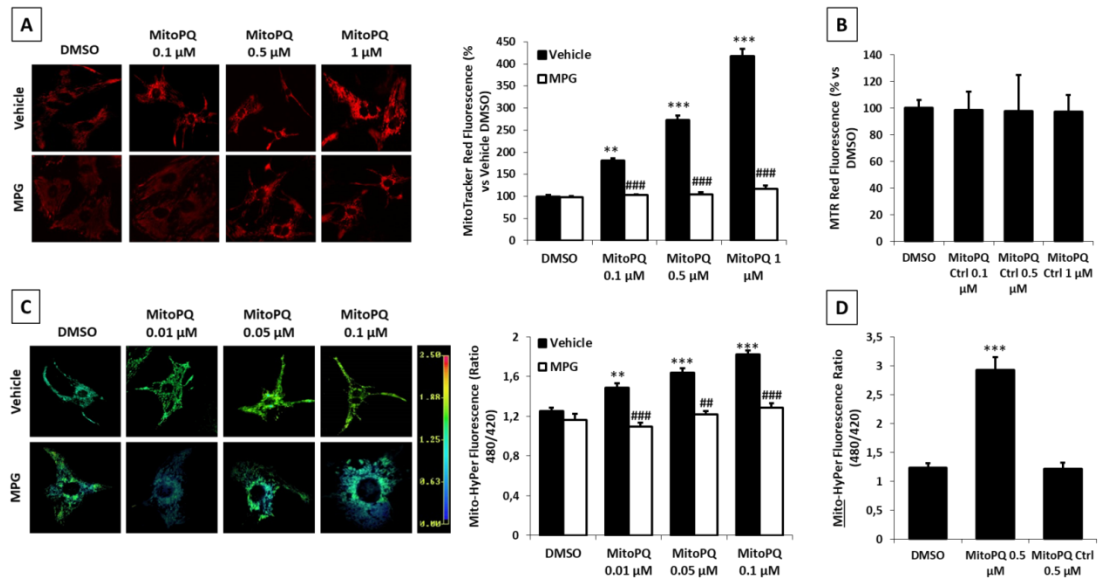
FIGURES

Figure 1. Effect of MitoPQ on ROS formation. Mitochondrial ROS formation monitored by: **A)** MTR in isolated NRVMs treated for 2 h with different concentrations of MitoPQ or **B)** MitoPQ Control Compound, with or without 30 min of pretreatment 500 μM MPG. Scale Bar: 30 μm. **C)** Mitochondrial H_2O_2 formation measured by MitoHyPer in isolated NRVMs treated for 2 h with different concentrations of MitoPQ, with or without 30 min of pretreatment with 500 μM MPG. Scale Bar: 20 μm **D)** Mitochondrial H_2O_2 formation measured by MitoHyPer in isolated NRVMs treated for 2 h with 0.5 μM MitoPQ or 0.5 μM MitoPQ Control Compound. Approximately 70 cells were analyzed per condition in each experiment and all the experiments were performed at least three times. Data are expressed as mean ± SEM. *p < 0.05, **p < 0.01, ***p < 0.001 vs DMSO vehicle; #p < 0.05, ##p < 0.01, ###p < 0.001 vs MitoPQ
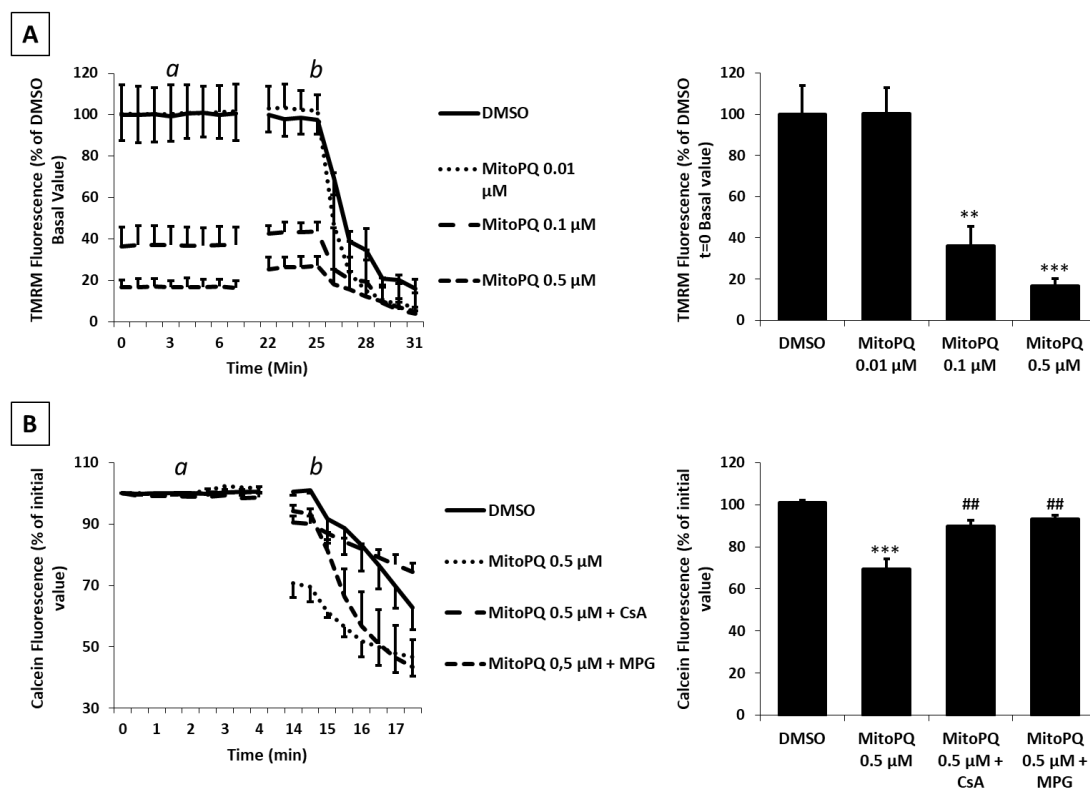
Figure 2. Effects of MitoPQ on mitochondrial membrane potential and mPTP opening. **A)** Mitochondrial membrane potential (ΔΨm) monitored by TMRM fluorescence in isolated NRVMs following incubation for 2 h with MitoPQ at different concentrations *a*: 4 μM oligomycin, *b*: 4 μM FCCP. **B)** mPTP opening monitored by decrease of calcein fluorescence in isolated NRVMs pretreated for 30 min with or without 1 μM CsA or 500 μM MPG. *a*: treatment with DMSO as control or 0.5 μM MitoPQ; *b*: 5 μM Calcimycin. Data were quantified 12 minutes after treatment with MitoPQ/DMSO. Approximately 30 cells were analyzed per condition in each experiment and all the experiments were performed at least three times. Data are expressed as mean ± SEM. *p < 0.05, **p < 0.01, ***p < 0.001 vs DMSO vehicle; #p < 0.05, ##p < 0.01, ###p < 0.001 vs MitoPQ

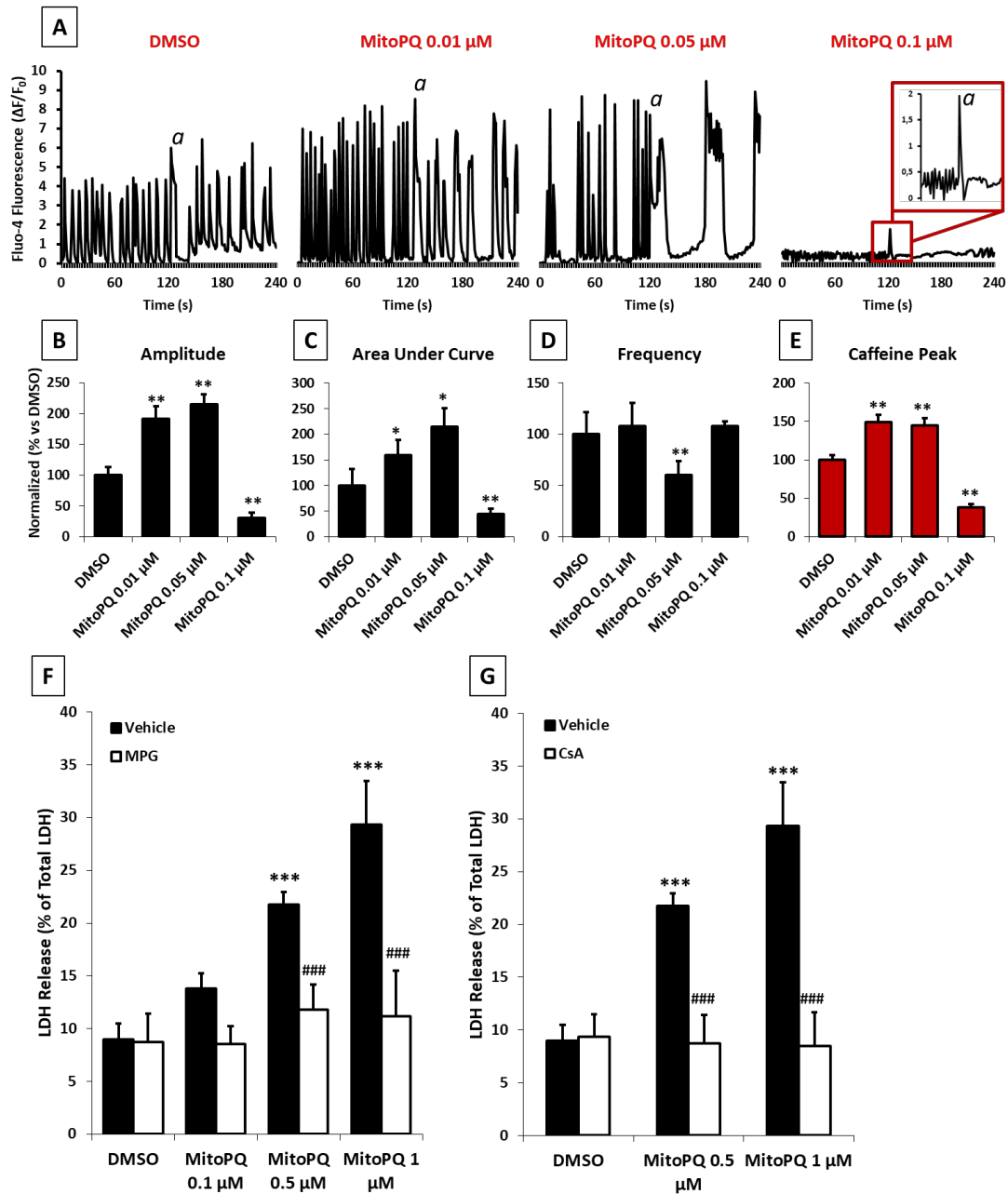**Figure 3. Effects of MitoPQ on cytosolic [Ca^{2+}] homeostasis and cell viability. A-E)** cytosolic [Ca^{2+}] homeostasis monitored by Fluo-4 AM in isolated NRVMs treated for 2 h with different concentrations of MitoPQ. **A)** Comparison between cytosolic Ca^{2+} oscillatory patterns. *a*: 10 mM caffeine. **B)** Peak amplitude average; **C)** Area Under Curve (AUC) average; **D)** Peaks Frequency average; **E)** Average caffeine Peak amplitude. **F-G)** Cell death monitored by LDH released from isolated NRVMs treated for 24 h with different concentrations of MitoPQ and pretreated with or without **F)** 500 μM MPG or **G)** 1 μM CsA. *A-E:* Approximately 30 cells were analyzed per condition in each experiment and all the experiments were performed at least three times. Data are expressed as mean ± SEM. *F-G:* Approximately 4 wells (cell density: 1.5x10^5 cells/well in 24 wells plates) were analyzed per condition in each experiment and all the experiments were performed at least three times. Data are expressed as mean ± SEM. *p < 0.05, **p < 0.01, ***p < 0.001 vs DMSO vehicle; #p < 0.05, ##p < 0.01, ###p < 0.001 vs MitoPQ
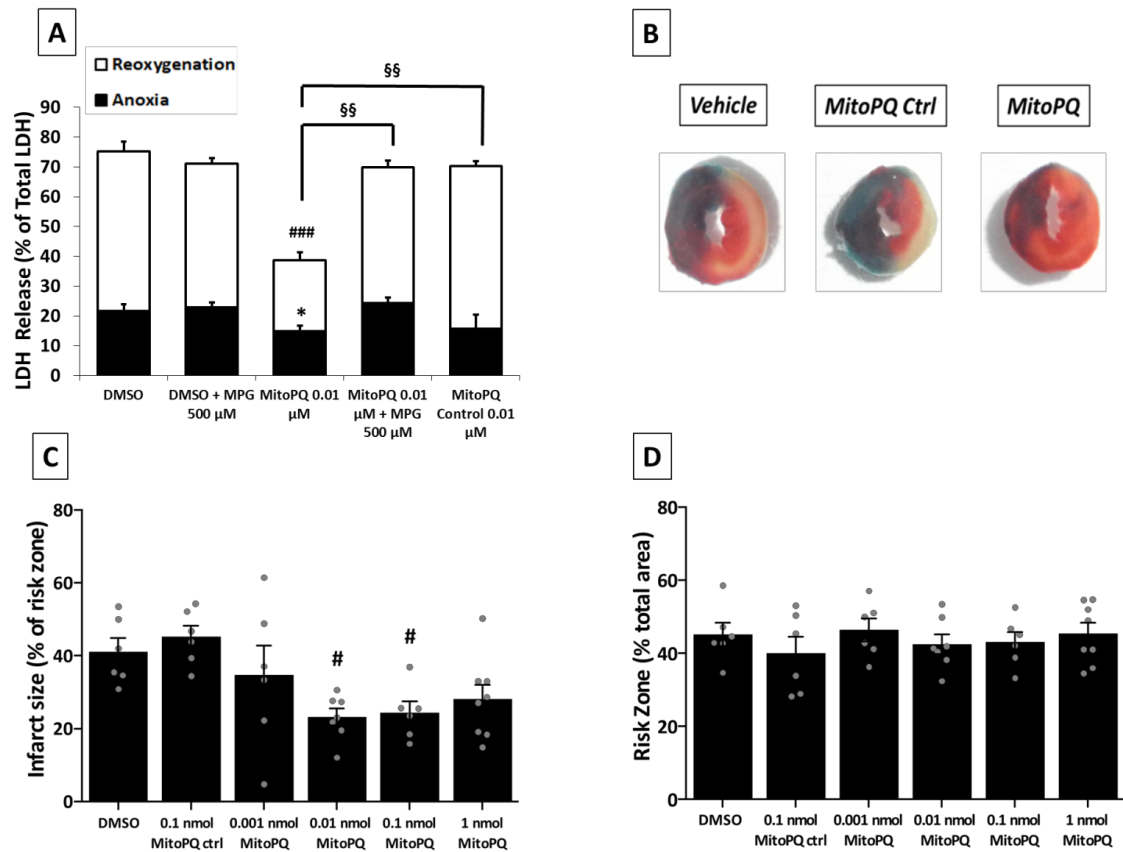
Figure 4. Effects of MitoPQ on cardiomyocytes viability both *in vitro* and *in vivo*. A) Cell death measured by LDH release from isolated NRVMs treated for 2 hours with 0.01 µM MitoPQ or 0.01 µM MitoPQ control compound, with or without 500 µM MPG. *p < 0.05 vs DMSO Anoxia, ###p < 0.001 vs DMSO Reoxygenation, §§p < 0.01 vs MitoPQ. **B)** Representative infarct slices from hearts treated with vehicle, MitoPQ control compound 0.01 nmol MitoPQ. **C)** Infarct size in hearts of mice exposed to acute myocardial I/R, in presence or absence of 0.01 nmol MitoPQ control compound or the indicated dose of MitoPQ. *p < 0.05 vs DMSO. **D)** Risk zone in heart of mice exposed to acute myocardial I/R, in presence or absence of 0.01 nM MitoPQ control compound or the indicated dose of MitoPQ. *A:* at least 4 wells (cell density: 1.5×10^5 cells/well in 24 wells plates) were analysed per condition in each experiment and all the experiments were performed at least three times. Data are expressed as mean ± SEM. *B-D: n = 6-8.* Data are expressed as mean ± SEM. #p < 0.05. Overall Anova p = 0.0053.

SUPPLEMENTARY TABLE AND FIGURES

|	Vehicle		MitoParaquat	
	mean fold change	SEM	mean fold change	SEM
Cardiac Output	1.17	0.15	1.13	0.22
Heart rate	1.00	0.00	0.98	0.00
Ejection fraction	1.00	0.04	0.99	0.05
Stroke Volume	1.17	0.15	1.15	0.23
End systolic volume	1.15	0.17	1.23	0.16
End diastolic volume	1.10	0.13	1.12	0.18
End systolic pressure	1.01	0.03	0.98	0.02
End diastolic pressure	1.32	0.34	1.30	0.28
Stroke Work	1.13	0.14	1.06	0.23
Mean pressure	1.05	0.05	1.02	0.04
Developed pressure	0.99	0.00	0.97	0.01
dP/dt_max	0.91	0.05	0.86	0.03
dP/dt_min	0.98	0.05	0.88	0.03
dV/dt_max	1.27	0.30	1.24	0.25
dV/dt_min	1.34	0.27	1.10	0.25
Pressure at dV/dt_max	1.03	0.23	1.08	0.28
Pressure at dP/dt_max	0.97	0.01	0.93	0.01
Volume at dP/dt_max	1.17	0.12	1.15	0.21
Volume at dP/dt_min	1.19	0.18	1.24	0.16

Table S1. MitoPQ does not affect haemodynamics. A closed chest experimental model was used to assess the effect of MitoPQ on haemodynamics. A pressure-volume catheter using admittance technology was inserted into the left ventricle via the right carotid artery. No significant difference in the fold change of values of any of the parameters measured following i.v. injection, compared between MitoPQ (0.1 nmol) or vehicle only. n = 4, Student's t-test with Bonferroni correction for multiple comparisons.
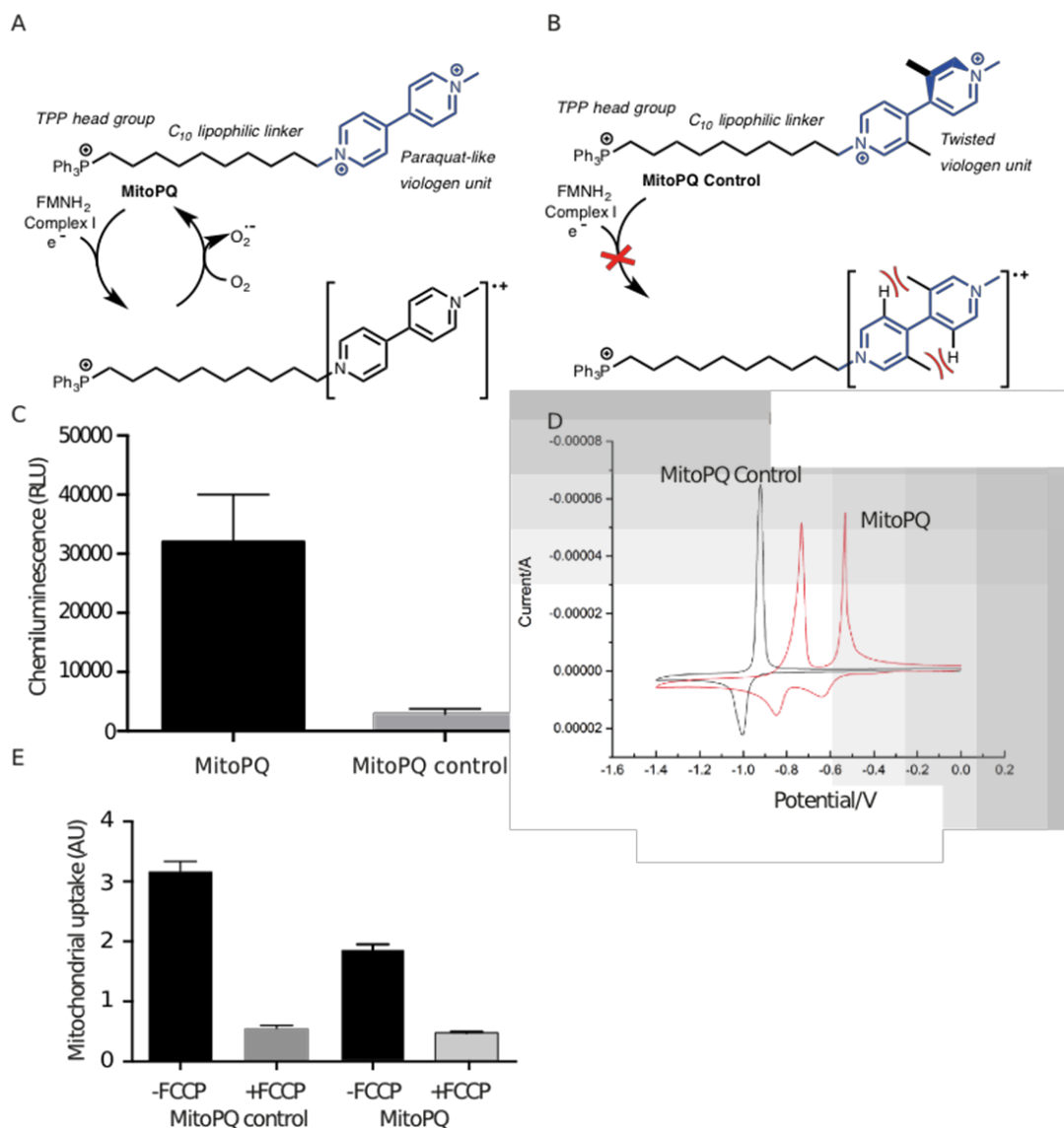
Supplementary Figure 1. Comparison of MitoPQ and MitoPQ Control. A) MitoPQ is comprised of an alkyltriphenylphosphonium (TPP) head group for targeting to the mitochondrial matrix, a lipophilic alkyl linker and a viologen head group similar to that of paraquat (spectator counterions omitted for clarity). The viologen is reduced by $FMNH_2$ of complex I to give the corresponding radical cation, in which the charge and radical character is delocalized over the two pyridine rings. Rapid reaction with molecular oxygen then produces superoxide and regenerates MitoPQ. **B)** The two methyl groups of MitoPQ control induce a twist in the viologen unit and the compound is less easily reduced because the coplanarity required for a delocalized radical cation is disfavoured. Thus, complex I is not sufficiently reducing to reduce MitoPQ control. **C)** *Superoxide production.* Bovine heart mitochondrial membranes (70 μg protein) were incubated in KCl buffer (120 mM KCl, 10 mM Hepes, 1 mM EGTA, pH 7.4) with 4 μg/ml rotenone, 2 μM coelentrazine and 1 mM NADH $\pm$ 1 μM MitoPQ or MitoPQ control in a 1 ml final volume. Coelentrazine luminescence was recorded on a Berthold Autolumat Plus luminometer at 30°C. **D)** *Cyclic voltammograms of MitoPQ and MitoPQ control ($1x10^{-3}$ M in pH 7.4 phosphate buffer).* The reference electrode was Ag/AgCl and was measured at scan rate of 0.05 V/s. The working electrode was a glassy carbon disk and the counter electrode was platinum wire. As expected from the literature (Andersson et al., 2009), while MitoPQ has a first reduction half potential of –0.59 V, MitoPQ control is much more difficult to reduce with a reduction half potential of –0.97 V in pH 7.4 phosphate buffer. **E)** *Uptake by isolated mitochondria.* Rat liver mitochondria (1 mg/ml) were incubated in KCl buffer (120 mM KCl, 10 mM Hepes, 1 mM EGTA) with succinate (10 mM), rotenone (4 μg/ml), TPMP (5 μM), and MitoPQ or MitoPQ control (5 μM) $\pm$ FCCP (0.5 μM) at 37°C for 5 min. The mitochondria were then pelleted by centrifugation (5 min at 10000 x g). The pellet was disrupted by vortexing with 250 μl of 99.9% ACN + 0.1% TFA and centrifuged again (5 min at 10000 x g). The supernatant was removed and added to 750 μl 99.9% water + 1% TFA and analysed by RP-HPLC with peak areas recorded.
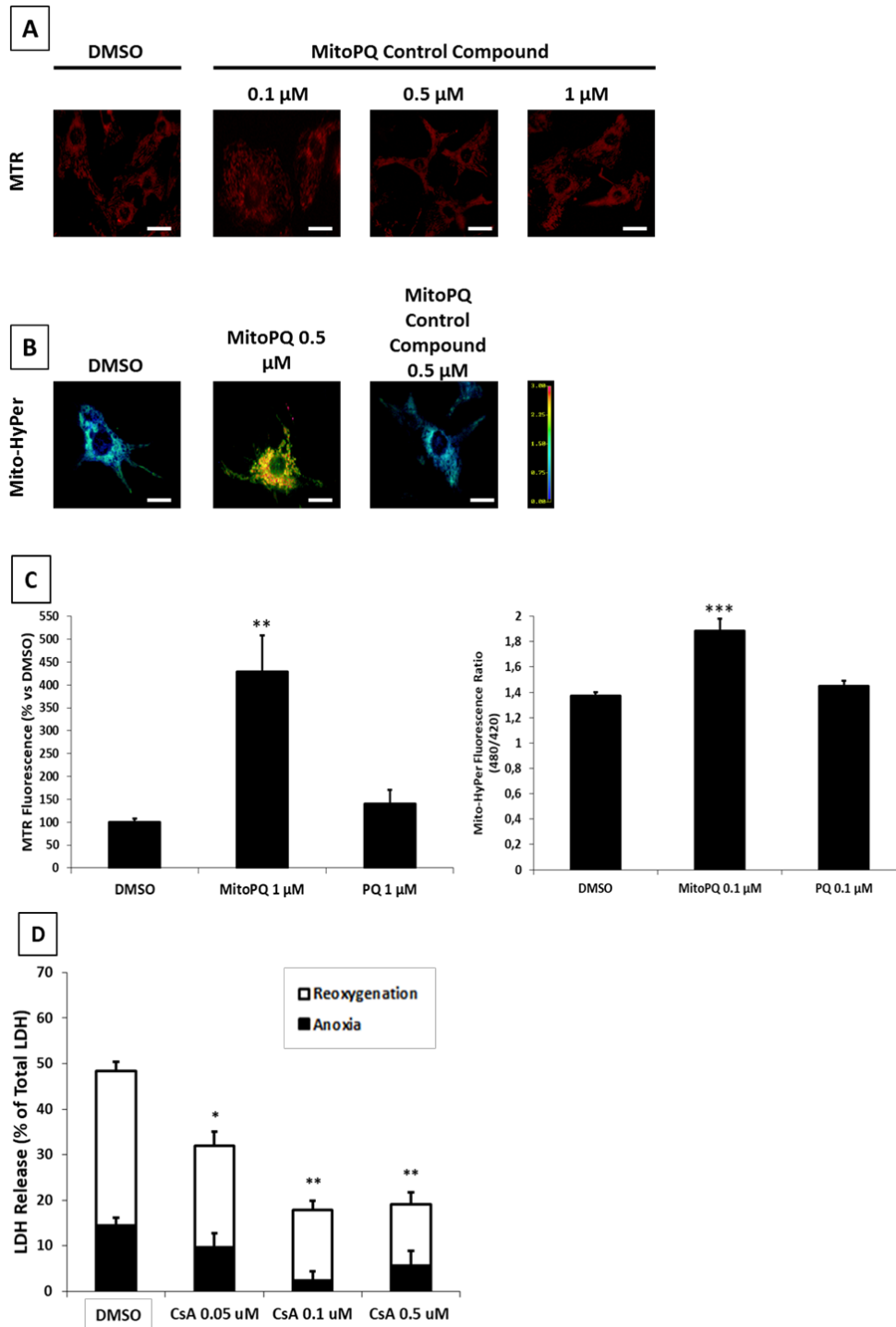
Supplementary Figure 2. Effect of MitoPQ Control Compound and PQ on ROS formation and effect of CsA in NRVMs exposed to A/R injury. A) Mitochondrial ROS formation monitored by MTR in isolated NRVMs treated for 2 h with different concentrations of MitoPQ Control Compound (0.1 – 0.5 – 1 μM). *Representative images. Scale Bar: 30 μm* **B)** Mitochondrial H_2O_2 formation measured by MitoHyPer in isolated NRVMs treated for 2 h with 0.5 μM MitoPQ or 0.5 μM MitoPQ Control Compound. *Representative images. Scale Bar: 20 μm* **C)** Mitochondrial ROS and H_2O_2 formation measured by MTR and MitoHyPer in isolated NRVMs treated for 2 h with different concentrations of MitoPQ (0.1 – 1 μM) or PQ (0.1 – 1 μM). **D)** Cell death measured by LDH release from isolated NRVMs exposed to 12 hours of anoxia and 1 hour of reoxygenation in presence or absence of different doses of CsA (0.05 – 0.1 – 0.5 μM). *p < 0.05, **p < 0.01 vs DMSO Reoxygenation.
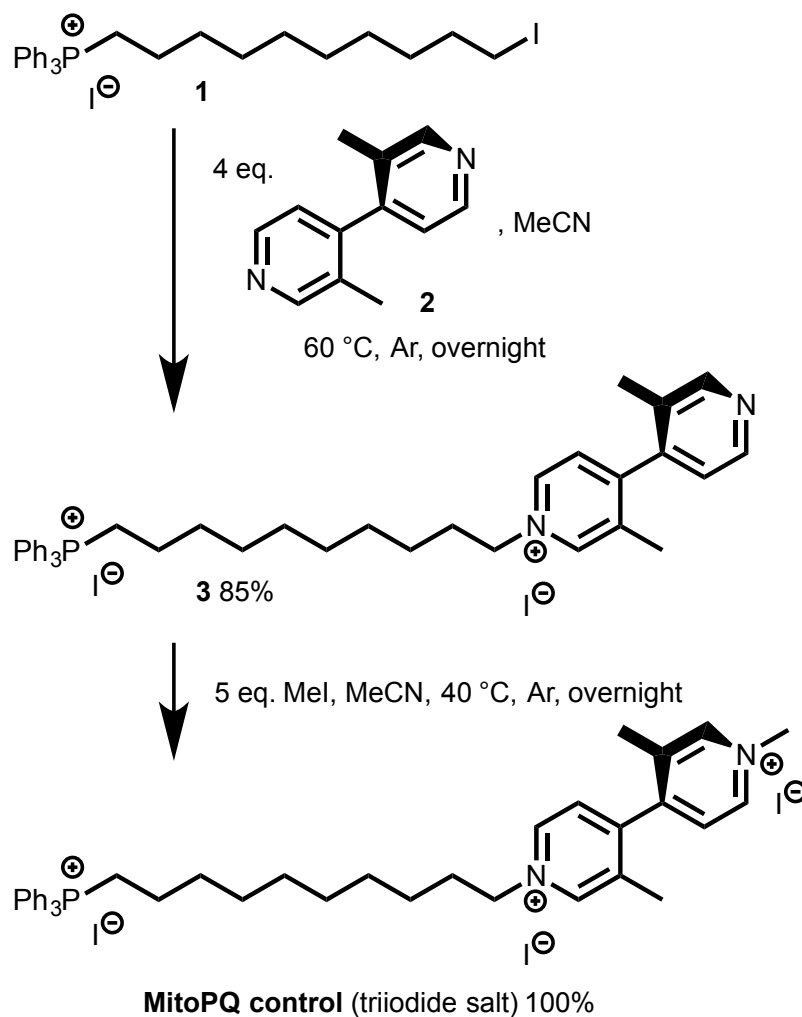
Supplementary Figure 3. Synthesis of MitoPQ control. MitoPQ was synthesized from iododecyl-TPP salt 1, which was prepared as described previously (Robb et al.). This was reacted with an excess of dimethyl-4,4'-dipyridyl 2, prepared by the procedure of (Rebek et al.), to minimise dialkylation. The monoalkylated product 3 was isolated in excellent year and was then methylated to give complete conversion to MitoPQ control.